Luo *et al. Biochar* (2026) 8:146
https://doi.org/10.1007/s42773-026-00660-6

Biochar

ORIGINAL RESEARCH Open Access

# Biochar and halophyte litter synergistically enhance recalcitrant organic carbon fractions in coastal salt-affected soil via lignin phenols and microbial necromass carbon

Xianxiang Luo[1,2*], Zhimeng Liang[1], Liuqingqing Liu[1,2*], Kun Chen[1,2], Lize Zhao[1,2], Qiang Liu[3], Zhengyang Wang[1], Yufei Cao[1], Fengmin Li[1,2] and Hao Zheng[1,2,3*]

## Abstract

Biochar shows promise for remediating coastal salt-affected soils and supporting potential carbon sequestration, yet its role in the halophyte litter detritusphere, particularly regarding lignin phenols and microbial necromass C (MNC), remains unclear. Herein, we conducted a 370-day microcosm experiment with coastal salt-affected soil from the Yellow River Delta under two moisture conditions (75% and 125% of maximum water-holding capacity) to evaluate how corn straw biochar (CBC) affects lignin phenols and MNC accumulation in the halophyte *Suaeda salsa* litter detritusphere. Results showed that CBC and litter inputs were stronger drivers of lignin phenol and MNC accumulation than moisture conditions. Litter input significantly increased the contents of lignin phenols and MNC by 32.80–33.36% and 0.78–14.36%, whereas CBC alone decreased lignin phenol content by 12.18–12.87%, but enhanced MNC accumulation by 15.36–42.22%. Compared with litter alone, CBC addition with litter significantly increased lignin phenols, bacterial necromass carbon (BNC), and MNC by 22.43–41.15%, 165.21–233.48%, and 25.09–53.82% under both moisture conditions. Mechanistically, CBC addition with litter alleviated salinity/sodicity stress and improved nutrient availability, enriching decomposition-associated taxa (*Preussia*, *Talaromyces*) and taxa associated with BNC accumulation (*Thiobacillus*, *Thioalkalispira*). Concurrently, CBC was associated with greater aggregate stability and organo-mineral associations, patterns that may favor the retention of lignin-derived residues and microbial necromass. These findings inform biochar as a nature-based strategy for sustainable management of coastal salt-affected soils and carbon sequestration.

## Highlights

- Biochar promotes plant-derived carbon and MNC accumulation in halophyte litter detritusphere.
- Biochar boosts MNC accumulation in detritusphere mainly through enhanced BNC.

*Correspondence:
Xianxiang Luo
lxx81875@ouc.edu.cn
Liuqingqing Liu
llqq@ouc.edu.cn
Hao Zheng
zhenghao2013@ouc.edu.cn
Full list of author information is available at the end of the article

© The Author(s) 2026. **Open Access** This article is licensed under a Creative Commons Attribution 4.0 International License, which permits use, sharing, adaptation, distribution and reproduction in any medium or format, as long as you give appropriate credit to the original author(s) and the source, provide a link to the Creative Commons licence, and indicate if changes were made. The images or other third party material in this article are included in the article's Creative Commons licence, unless indicated otherwise in a credit line to the material. If material is not included in the article's Creative Commons licence and your intended use is not permitted by statutory regulation or exceeds the permitted use, you will need to obtain permission directly from the copyright holder. To view a copy of this licence, visit http://creativecommons.org/licenses/by/4.0/.

Springer

- Biochar remediation is associated with enhanced SOC retention and indicators of aggregate and mineral protection in the detritusphere.

**Keywords** Soil health, Detritusphere, Carbon storage, Lignin-derived compounds, Remediation

**Graphical Abstract**

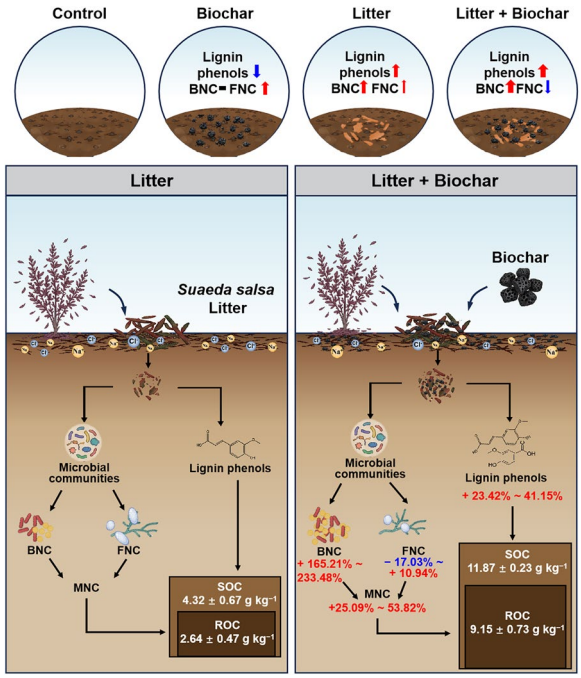


## 1 Introduction

Healthy soils are fundamental to food security and climate mitigation, yet salt-affected soils now occupy approximately $1.0 \times 10^9$ $hm^2$ globally, of which more than 10% is potentially cultivable (Negacz et al. 2022). Bringing this land into productive use offers a tangible pathway to alleviate cropland shortages and secure future food supply. Coastal salt-affected lands, in particular, are tightly linked to blue-carbon ecosystems and thus hold relevance for climate-change mitigation (Macreadie et al. 2021). In the Yellow River Delta, ongoing salinization has been accompanied by declining soil carbon (C) stocks (Chen et al. 2019; Tang et al. 2024). With the national strategies for Yellow River Basin protection and the dual-carbon targets gaining momentum, enhancing soil health and C sequestration in this region has become an urgent priority (Wang et al. 2023). There is a clear need for nature-based, low-carbon approaches that can simultaneously support land restoration and C sequestration.

Biochar is widely regarded as a negative-emission technology that enhances soil C storage by introducing persistent C inputs and modifying soil C pool dynamics (Lehmann et al. 2021; Liu et al. 2023; Zheng et al. 2018a). Consequently, biochar has been increasingly adopted for remediation and C sequestration in coastal salt-affected soils, including those of the Yellow River Delta (Zhang et al. 2021; Yu et al. 2021). In these environments, biochar improves soil quality and functionality by lowering bulk density and salinity, enhancing nutrient availability, and stimulating microbial activity, changes that collectively promote plant productivity and the accumulation of stable C (Zhang et al. 2021; Zheng et al. 2018b). However, the persistence and stability of biochar-induced soil organic C (SOC) gains depend critically on the subsequent transformation and protection of both plant-derived and microbial-derived C. In particular, the role of biochar in influencing microbial necromass C accumulation, a key contributor to stable SOC pools, and its interaction with plant-derived C inputs in salt-affected detritusphere systems remain poorly understood. Clarifying these mechanisms is therefore essential

for evaluating the true potential of biochar to improve coastal salt-affected soils and deliver durable C sequestration benefits.

Lignin phenols and microbial necromass C (MNC) are major contributors to SOC in salt-affected soils (Li et al. 2023b). Lignin phenols are aromatic intermediates of lignin degradation and are widely used as molecular tracers of plant-derived C dynamics in soil (Thevenot et al. 2010). MNC comprises bacterial necromass C (BNC) and fungal necromass C (FNC), both of which can be stabilized through aggregate occlusion and organo-mineral associations once formed, thereby contributing substantially to persistent SOC pool. In the coastal salt-affected soils of the Yellow River Delta, MNC accounts for approximately 10.40–25.40% of SOC (Shao et al. 2022). To date, however, research in these systems has largely focused on quantifying MNC stocks (Chen et al. 2021; Li et al. 2023b; Shao et al. 2022), with less attention given to how management practices such as biochar application affect its accumulation. Recent studies suggest that biochar can alter MNC accumulation during salt-affected soil remediation, though the reported effects vary considerably. For instance, annual application of rice-straw biochar at 4 or 8 t $ha^{-1}$ significantly increased FNC in salt-affected cropland soils of the Yellow River Delta (Wang et al. 2025b), whereas maize-straw biochar significantly increased both BNC and FNC in coastal salt-affected cropland (Cheng et al. 2024). In a coastal afforestation site, rice-husk biochar significantly increased BNC but not FNC (Wang et al. 2025a). These findings indicate that biochar effects on MNC components are context-dependent, varying with biochar type, land use, and site conditions. What remains unclear, however, is whether corn straw biochar (CBC) influences BNC and FNC accumulation, and hence total MNC, when native halophyte litter is present, a scenario that is ecologically relevant for detritusphere processes in coastal salt-affected soils.

The detritusphere, the interface between litter and mineral soil, is a hotspot of C dynamics centered on plant residues (Kuzyakov and Blagodatskaya 2015). With litter as the substrate and microorganisms as the primary decomposers, this micro-zone drives intensive C turnover (Vidal et al. 2021). Litter inputs can accelerate decomposition and transformation by increasing microbial C use efficiency (CUE) and promoting microbial growth and turnover, processes that generate microbial necromass and stable metabolites, thereby facilitating soil organic C (SOC) accumulation (Qiao et al. 2025; Liu et al. 2025). Microbial hyphae and extracellular polymeric substances further facilitate the transfer of newly formed organic matter to mineral surfaces, where it becomes stabilized through physical occlusion within aggregates and organo-mineral associations (Elias et al. 2024; Vidal et al. 2021; Witzgall et al. 2021). Collectively, these studies suggest that plant-derived lignin phenols and MNC operate synergistically and complementarily during long-term SOC accumulation, jointly driving SOC sequestration (Li et al. 2023c). Previous work has also shown that biochar can accelerate litter decomposition and transformation, and promote the conversion of plant-derived C into microbial-derived C, by improving soil structure, nutrient availability, and microbial activity (Cui et al. 2017; Minamino et al. 2019; Vannini et al. 2023). Thus, biochar may regulate SOC accumulation by reshaping the coupling between plant-derived lignin phenol inputs and microbial necromass accumulation. However, most current evidence comes from non-salt-affected soils (Bai et al. 2024; Chen et al. 2024). It therefore remains unclear how biochar input affects the accumulation of lignin phenols and MNC in the detritusphere, and how their coupling contributes to SOC accumulation and stabilization in coastal salt-affected soils—where compacted structure, low nutrient availability, and severe salinization impose strong constraints on microbial activity and C turnover.

In previous work, we established a microcosm system simulating the halophyte litter-soil interface in coastal salt-affected soil with biochar addition, and demonstrated that biochar effectively regulated phosphorus (P) availability and associated microbial processes under different moisture regimes (Luo et al. 2024). However, that study did not address the transformation and accumulation of C fractions at the litter-soil interface. Building on this system, the present study conducted a 370-day incubation experiment to examine how CBC input affects lignin phenols and MNC accumulation in the *Suaeda salsa* detritusphere under two moisture conditions (75% and 125% water-holding capacity) using typical coastal salt-affected soil from the Yellow River Delta, northern China. The specific objectives were to: (1) quantify litter decomposition and lignin phenol accumulation; (2) characterize MNC formation and microbial community assembly; and (3) evaluate synergistic effects on SOC stabilization. Together, these findings are expected to inform the design of green remediation and land-management strategies that jointly enhance soil health and C sequestration in coastal salt-affected lands.

## 2 Materials and methods

### 2.1 Soil and litter sampling

Surface soil (0–20 cm) was collected from a coastal salt-affected land in the Yellow River Delta near Xianhe Town, Dongying, China (38° 11′ N, 118° 43′ E). Soil pretreatment procedures and properties were described in our previous study (Luo et al. 2024) and are summarized in

Table S1. *Suaeda salsa*, a native pioneer halophyte in this region, was collected in November from Qingfeng Lake Park, Dongying (37° 24′ N, 118° 40′ E). The collected litter was air-dried, sieved to 0.25–2.00 mm, and stored. Its properties are provided in Table S2.

### 2.2 Preparation and characterization of corn straw biochar

CBC was previously produced by slow pyrolysis at 450 °C for 5 h under $N_2$ atmosphere in a tube furnace (O-KTF1200, Chunlei, China) (Luo et al. 2024). Its properties are provided in Table S1. CBC morphology was examined by scanning electron microscopy (SEM, EVO10, Carl Zeiss, Germany), with representative images shown in Fig. S1.

### 2.3 Microcosm experiment

To simulate C turnover processes in coastal salt-affected soils under contrasting hydrological regimes, we established two moisture levels: 75% and 125% of maximum water-holding capacity (WHC), representing non-flooded and flooded conditions, respectively (Qu et al. 2021). The microcosm experiment was conducted in plastic containers each containing 1000 g of the prepared soil. Soil and CBC were sieved to 2.00 mm, and litter was sieved to 0.25–2.00 mm to standardize litter particle size and reduce sample heterogeneity (Xie et al. 2022). CBC was thoroughly mixed with air-dried soil at 3% (w/w, dry-weight basis) where applicable. For litter addition, 2.00 g of oven-dried litter was enclosed in a 150-mesh nylon litter bag (0.1 mm thick, 8 × 8 cm) and horizontally buried at 2.00 cm depth (Hu et al. 2026), allowing microorganisms to access and decompose the litter while enabling full recovery of litter residues (Su et al. 2022; Yan et al. 2026). Four treatments were included under each moisture condition: (1) unamended soil (CK); (2) soil amended with CBC (BC); (3) soil amended with *Suaeda salsa* litter (SS); and (4) soil amended with both CBC and litter (BSS). Further details are provided in our previous study (Luo et al. 2024). The application rate (3%) of CBC was selected based on earlier incubation studies in the Yellow River Delta coastal salt-affected soils and its favorable performance for SOC sequestration (Luo et al. 2024). *Suaeda salsa* litter input in these soils ranges from 46.25 to 579.90 g $m^{-2}$ (Sun et al. 2013). Here, 2.00 g litter addition rate corresponded to approximately 312.50 g $m^{-2}$, falling within this range and thus approximating field-relevant conditions while ensuring a stable, reproducible detritusphere interface.

The microcosm incubation lasted for 370 days. Under each moisture condition, 15 independent incubation units were established for each litter-containing treatment (SS and BSS). On days 10, 100, 190, and 280, three independent incubation units from each treatment were randomly selected, and the residual litter bags were retrieved, freeze-dried, and stored for litter mass loss analysis (Text S2). On day 370, the remaining three independent incubation units were destructively sampled, and the residual litter was collected, together with detritusphere soil attached to and surrounding the litter bags within approximately 5 mm. For the treatments without litter bags (CK and BC), three independent incubation units were established under each moisture condition. On day 370, bulk soil was destructively collected from the position and depth corresponding to the litter bag burial layer as a position-matched bulk soil control (Text S3). The CK and BC treatments lacked litter input and therefore did not contain a strictly defined detritusphere. Detritusphere soil from the SS and BSS treatments was compared with position-matched bulk soil controls without litter influence to assess the effects of litter input (Kuzyakov and Blagodatskaya 2015; Yang et al. 2025). A portion of the collected soil was placed in cryovials and immediately stored at −80 °C for microbial analyses; another portion was air-dried for mean weight diameter (MWD) measurement; and the remaining air-dried soil was passed through a 100-mesh sieve and stored for property determination. Surface functional groups of initial oven-dried litter and 370-day residues were characterized by Fourier transform infrared (FTIR, Tensor 27, Bruker, Germany) (Zhang et al. 2025b).

### 2.4 Soil sample analyses

SOC and total nitrogen (TN) were determined using an elemental analyzer (Flash 2000, Thermo Scientific, USA). For SOC analysis, soil samples were pretreated with 5% HCl to remove inorganic C (Zheng et al. 2018b). Labile organic C (LOC) was determined by dichromate oxidation, and recalcitrant organic C (ROC) was calculated as the difference between SOC and LOC (Text S4) (Benslama et al. 2024; Nelson and Sommers 1996; Ramos et al. 2025).

Lignin phenols, including cinnamyl, vanillyl, and syringyl phenols, were quantified using the alkaline CuO oxidation method (Ma et al. 2020). Detailed procedures are provided in Text S5. The extent of lignin degradation was assessed using the acid-to-aldehyde ratios of vanillyl and syringyl phenols, (Ad/Al)v and (Ad/Al)s (Thevenot et al. 2010). MNC was quantified based on amino sugar biomarkers (Joergensen 2018). Glucosamine (GluN), galactosamine (GalN), and muramic acid (MurA) were measured by gas chromatography after aldononitrile acetate derivatization (Zhang and Amelung 1996; Text S6). BNC and FNC were estimated from MurA and GluN using established conversion factors, and MNC was calculated as BNC plus FNC (Meng et al. 2025; Text S7).

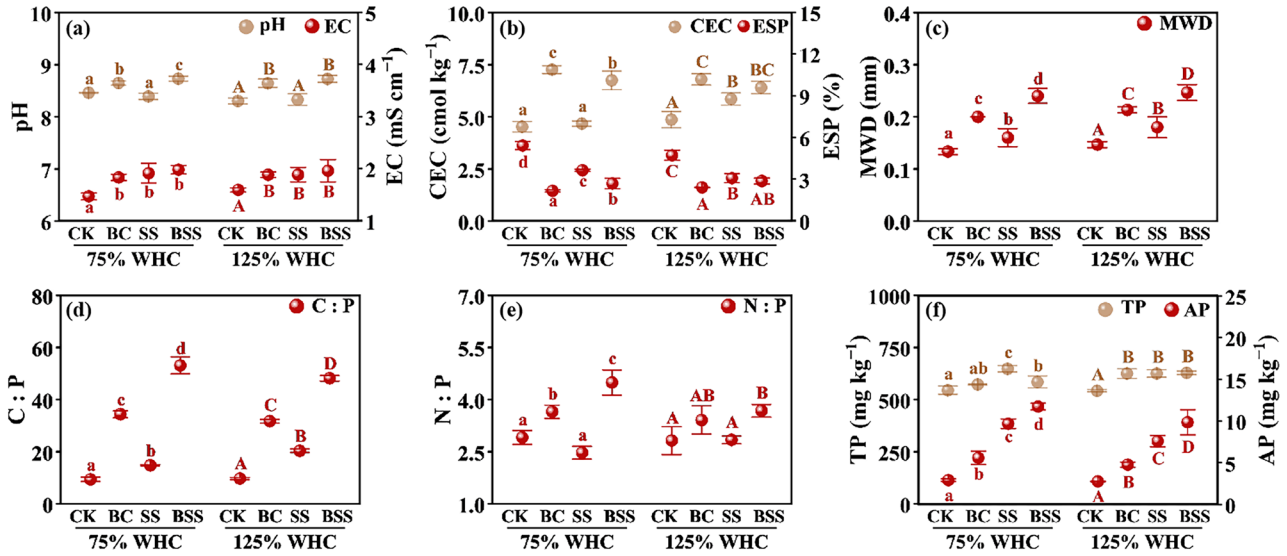


**Fig. 1** Changes in soil physicochemical properties. **a** pH and EC. **b** CEC and ESP. **c** MWD. **d** C:P ratio. **e** N:P ratio. **f** TP and AP. CK, unamended soil (control); BC, soil + CBC; SS, soil + litter; and BSS, soil + CBC + litter. Different lowercase and uppercase letters indicate significant differences among treatments at 75% and 125% water-holding capacity (WHC), respectively ($P < 0.05$)

Mineral- associated organic C fractions were determined using a sequential extraction method (Huang et al. 2020; Text S8).

Soil cation exchange capacity (CEC) and exchangeable Na (Ex-Na) were measured by ammonium acetate extraction, and exchangeable sodium percentage (ESP) was calculated from CEC and Ex-Na (Zheng et al. 2018b). Soil aggregate size distribution was measured by wet sieving (Rabbi et al. 2014), and aggregate stability was evaluated as the MWD of water-stable aggregates (Rabbi et al. 2014). Soil pH, EC, total P, and available P (AP) were measured using standard methods (Text S9).

### 2.5 Microbial community composition analysis

To elucidate the potential microbial mechanisms underlying changes in detritusphere C pools after 370 days of incubation, microbial community sequencing was performed on detritusphere soil samples from the SS and BSS treatments under both moisture regimes. Triplicate samples from each treatment were subjected to DNA extraction, and bacterial 16S rRNA gene and fungal ITS region sequencing were used to assess community composition. Methodological details are provided in Text S10.

### 2.6 Statistical analysis

Data are presented as the mean ± standard deviation, with three independent biological replicates for each treatment or sampling time point ($n = 3$). Statistical analyses were performed using IBM SPSS Statistics 27.0 (IBM SPSS, USA). Differences among treatment means were analyzed by one-way analysis of variance (ANOVA), followed by Duncan's multiple range test at $P < 0.05$, whereas differences between two groups were assessed using independent-samples *t* tests. Two-way ANOVA tested the main and interactive effects of biochar addition and moisture conditions on litter mass loss, whereas three-way ANOVA evaluated those of biochar addition, litter input, and moisture conditions on detritusphere C variables (Text S11). Spearman correlations were calculated in GraphPad Prism 10 (GraphPad Software, USA) and visualized as heatmaps. Microbial $\beta$-diversity was assessed using Bray–Curtis distances and visualized by PCoA. Principal component analysis (PCA) was used to summarize variation in lignin phenols and MNC. Details of multivariate analyses and Mantel tests are provided in Texts S12–S13.

## 3 Results

### 3.1 Changes in soil physicochemical properties

Under both moisture conditions, pH, EC, and CEC were significantly higher in BC and BSS than in CK ($P < 0.05$; Fig. 1a, b). By contrast, ESP was significantly lower and MWD was significantly higher in BC, SS, and BSS than in CK ($P < 0.05$; Fig. 1b, c). The C:P and N:P ratios in CK ranged from 8.79 to 10.37 and from 2.39 to 3.18, respectively (Fig. 1d, e). Relative to CK, C:P ratio increased significantly in BC, SS, and BSS, with the highest values observed in BSS ($P < 0.05$; Fig. 1d), whereas N:P ratio increased by 23.19% and 42.89% in BC and BSS, respectively ($P < 0.05$; Fig. 1e). Notably, in BSS, C:P and N:P ratios ranged from 47.25 to 56.06 and from 3.54 to 4.86,

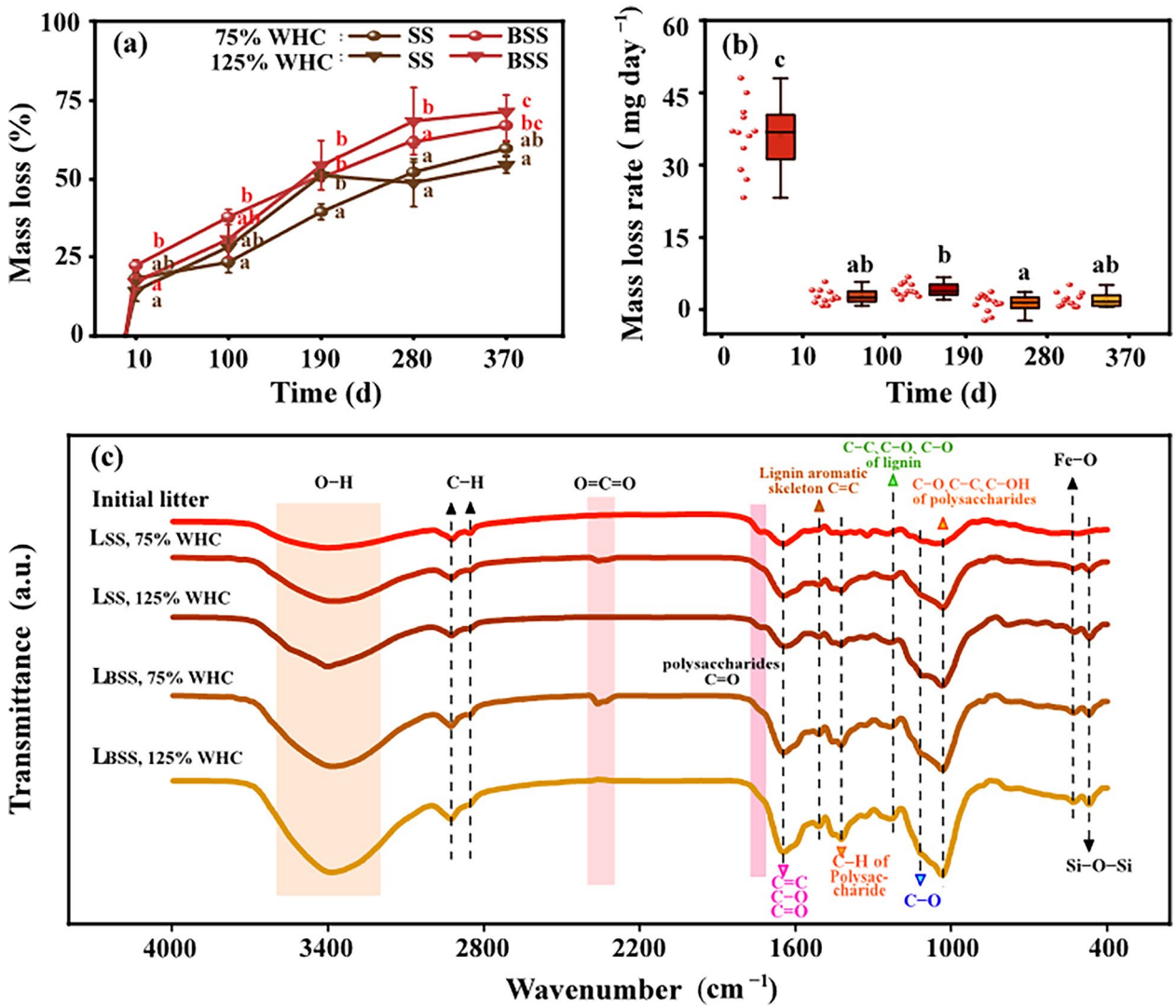


**Fig. 2** Litter decomposition dynamics and FTIR spectra. **a** Temporal changes in litter mass loss. **b** Temporal changes in litter mass loss rate. **c** FTIR spectra of initial litter and litter residues after 370 days of incubation. SS, soil + litter; BSS, soil + CBC + litter. Initial litter refers to the pretreated litter before incubation. $L_{SS,\ 75\%\ WHC}$ and $L_{SS,\ 125\%\ WHC}$ represent the litter residues from the SS treatment under 75% and 125% WHC, respectively; $L_{BSS,\ 75\%\ WHC}$ and $L_{BSS,\ 125\%\ WHC}$ represent litter residues from the BSS treatment under 75% and 125% WHC, respectively. Different lowercase letters indicate significant differences among treatments at the same sampling time ($P < 0.05$)

respectively, under both moisture conditions (Fig. 1d, e). Relative to CK, AP content increased by 204.95%, 82.68%, and 281.20% in BC, SS, and BSS ($P < 0.05$; Fig. 1f).

### 3.2 Decomposition dynamics and functional group transformations of litter

The dynamics of *Suaeda salsa* litter mass loss and the FTIR spectra are shown in Fig. 2. Over the 370-day incubation, cumulative litter mass loss ranged from 51.68% to 77.27% across treatments (Fig. 2a). Under both moisture conditions, litter mass loss was consistently higher in BSS than in SS, with a final increase of 16.39% relative to SS (Fig. 2a). The decomposition rate peaked during the initial 0–10 days and declined markedly thereafter ($P < 0.05$; Fig. 2b).

FTIR spectra revealed a preferential loss of labile components and relative enrichment of aromatic structures, with more pronounced changes in BSS than in SS (Fig. 2c). Bands associated with lignin and aromatic moieties intensified markedly in the residual litter, particularly at 1645 $cm^{-1}$ (aromatic C=C and carboxyl C=O), 1515 $cm^{-1}$ (lignin aromatic skeletal vibrations), 1475 $cm^{-1}$ (C–H bending), 1215 $cm^{-1}$ (lignin-related C–O/C–C/C=O), and 1080 $cm^{-1}$ (C–O–C vibrations).

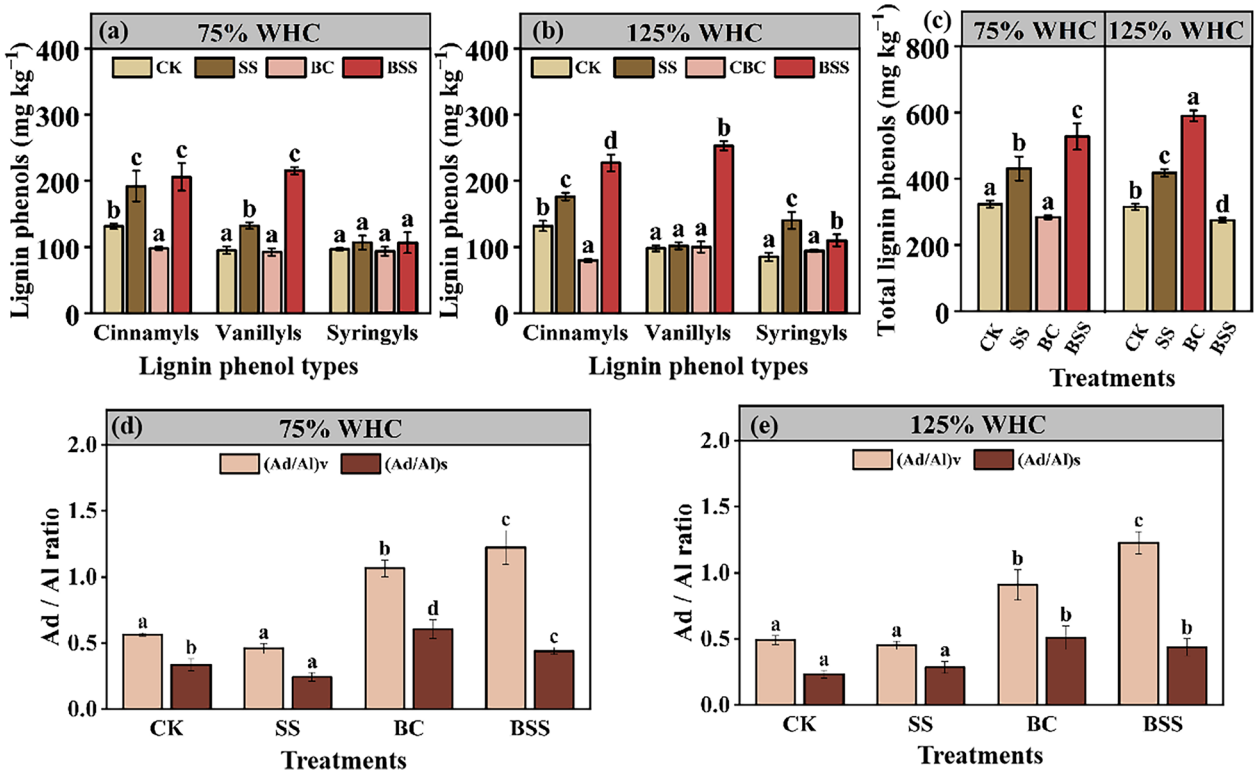


**Fig. 3** Lignin phenol contents and acid-to-aldehyde ratios. **a**, **b** Cinnamyl, vanillyl, and syringyl contents under 75% WHC and 125% WHC, respectively. **c** Total lignin phenols contents under 75% WHC and 125% WHC. **d**, **e** Vanillyl acid-to-aldehyde ratio (Ad/Al)v and syringyl acid-to-aldehyde ratio (Ad/Al)s under 75% WHC and 125% WHC, respectively. CK, unamended soil (control); BC, soil + CBC; SS, soil + litter; and BSS, soil + CBC + litter. Different lowercase letters indicate significant differences among treatments within each moisture condition ($P < 0.05$)

In addition, new bands appeared at 530 cm$^{-1}$ and 470 cm$^{-1}$, consistent with Fe–O and Si–O–Si vibrations, suggesting incorporation of mineral components during decomposition. Conversely, signals in the 1760–1700 cm$^{-1}$ region, typically assigned to hemicellulose and aliphatic ester groups (e.g., fatty acid esters), decreased substantially, indicating preferential loss of labile esterified components (Fig. 2c). Relative to SS, BSS residues exhibited consistently stronger intensities at 3600–3300 cm$^{-1}$, 1645 cm$^{-1}$, 1515 cm$^{-1}$, 1475 cm$^{-1}$, and 1080 cm$^{-1}$, further confirming enhanced decomposition and aromatic enrichment under biochar addition.

### 3.3 Lignin phenol contents and degradation indicators

Lignin phenol composition and acid-to-aldehyde ratios are summarized in Fig. 3. Lignin phenol contents increased with litter input and were further enhanced by CBC addition under both moisture conditions ($P < 0.05$; Fig. 3a–c). Taking the 125% WHC condition as an example, the contents of cinnamyl, syringyl, and total lignin phenols were significantly higher in SS and BSS than in CK ($P < 0.05$). Compared with SS, BSS increased the contents of cinnamyl, vanillyl, and total lignin phenols by 28.94%, 158.19%, and 41.15%, respectively ($P < 0.05$; Fig. 3b, c).

Under both moisture conditions, SS exhibited the lowest (Ad/Al)v and (Ad/Al)s ratios, whereas both ratios were significantly higher in BC and BSS than in CK and SS ($P < 0.05$). Relative to CK, the (Ad/Al)v increased by 86.92% in BC and 132.07% in BSS ($P < 0.05$), while the (Ad/Al)s increased by 95.91% in BC and 53.81% in BSS ($P < 0.05$). Compared with BC, BSS further increased the mean (Ad/Al)v by 24.15% but decreased the (Ad/Al)s by 21.49% ($P < 0.05$, Fig. 3d, e).

### 3.4 Amino sugars and microbial necromass carbon (MNC)

Amino sugars, MNC, GluN/MurA, and BNC/MNC are shown in Fig. 4. Under 75% WHC, MurA content showed little variation among CK, SS, and BC. Under 125% WHC, MurA content in SS was 14.21% higher than in CK ($P < 0.05$), though no significant difference was observed between BC and CK. Under both moisture conditions, MurA content was significantly higher in BSS than in CK, BC, and SS, with increases of 283.68%, 216.56%, and 215.57%, respectively (Fig. 4a, b). Under both moisture conditions, GluN content in BC was 28.46% higher than

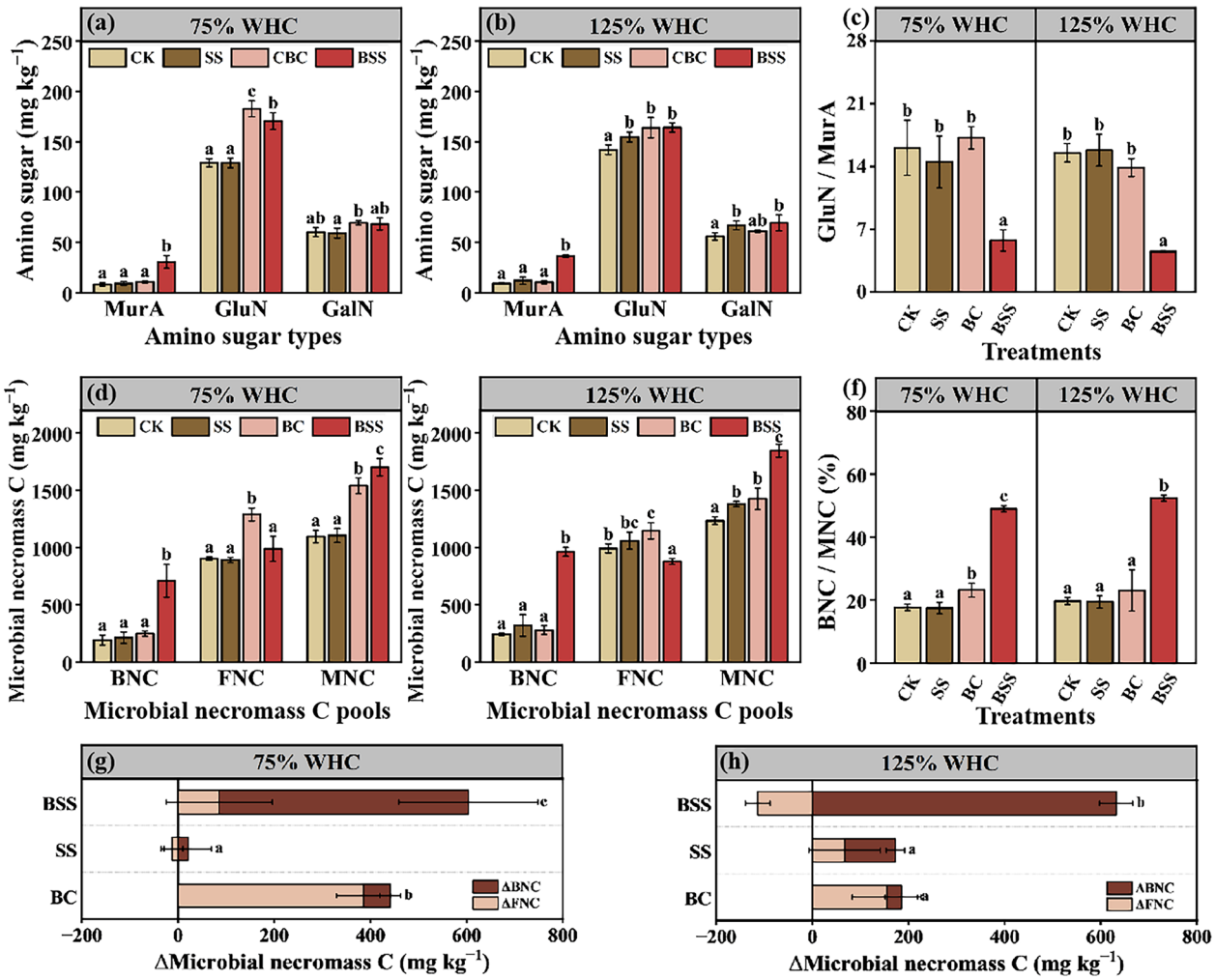


**Fig. 4** Changes in amino sugars contents, microbial necromass C pools, related ratios, and increments in microbial necromass C relative to CK. **a**, **b** MurA, GluN, and GalN contents under 75% WHC and 125% WHC, respectively. **c** GluN/MurA ratio under 75% WHC and 125% WHC **d**, **e** BNC, FNC, and MNC contents under 75% WHC and 125% WHC, respectively. **f** BNC/MNC ratio under 75% WHC and 125% WHC. **g**, **h** Increments in BNC, FNC, and MNC relative to CK (ΔBNC, ΔFNC, and ΔMNC) under 75% WHC and 125% WHC, respectively. CK, unamended soil (control); BC, soil + CBC; SS, soil + litter; and BSS, soil + CBC + litter. Different lowercase letters indicate significant differences among treatments within each moisture condition ($P < 0.05$)

in CK ($P < 0.05$), whereas SS significantly increased GluN content by 8.96% only under 125% WHC. GluN content in BSS was significantly increased by 23.86% relative to CK ($P < 0.05$; Fig. 4a, b). The GluN/MurA ratio in BSS was significantly lower than in CK, BC, and SS by 67.51%, 68.90%, and 63.11%, respectively ($P < 0.05$; Fig. 4c).

Under both moisture conditions, BNC content in BSS was significantly higher than in CK, BC, and SS by 283.58%, 216.53%, and 192.56%, respectively ($P < 0.05$; Fig. 4d, e). Under both moisture conditions, FNC content in BC was significantly higher than in CK and BSS by 28.49% and 30.38%, respectively ($P < 0.05$; Fig. 4d, e), and under 75% WHC, it was also significantly higher than in SS by 44.53% ($P < 0.05$; Fig. 4d). Under both moisture conditions, MNC content in BSS was significantly higher than in CK, BC, and SS by 48.75%, 16.94%, and 37.87%, respectively ($P < 0.05$; Fig. 4d, e). Under 75% WHC, MNC content in BC was significantly higher than in CK and SS by 40.22% and 39.13%, respectively ($P < 0.05$; Fig. 4d). Under 125% WHC, MNC content in BC and SS was significantly higher than in CK by 15.36% and 14.36%, respectively ($P < 0.05$; Fig. 4e). The BNC/MNC ratio in BSS was 158%, 170%, and 114% higher than that in CK, BC, and SS, respectively ($P < 0.05$; Fig. 4f). Relative to CK, the mean increase in MNC (ΔMNC) in BSS exceeded the sum of the mean ΔMNC in BC and SS ($P < 0.05$). Across

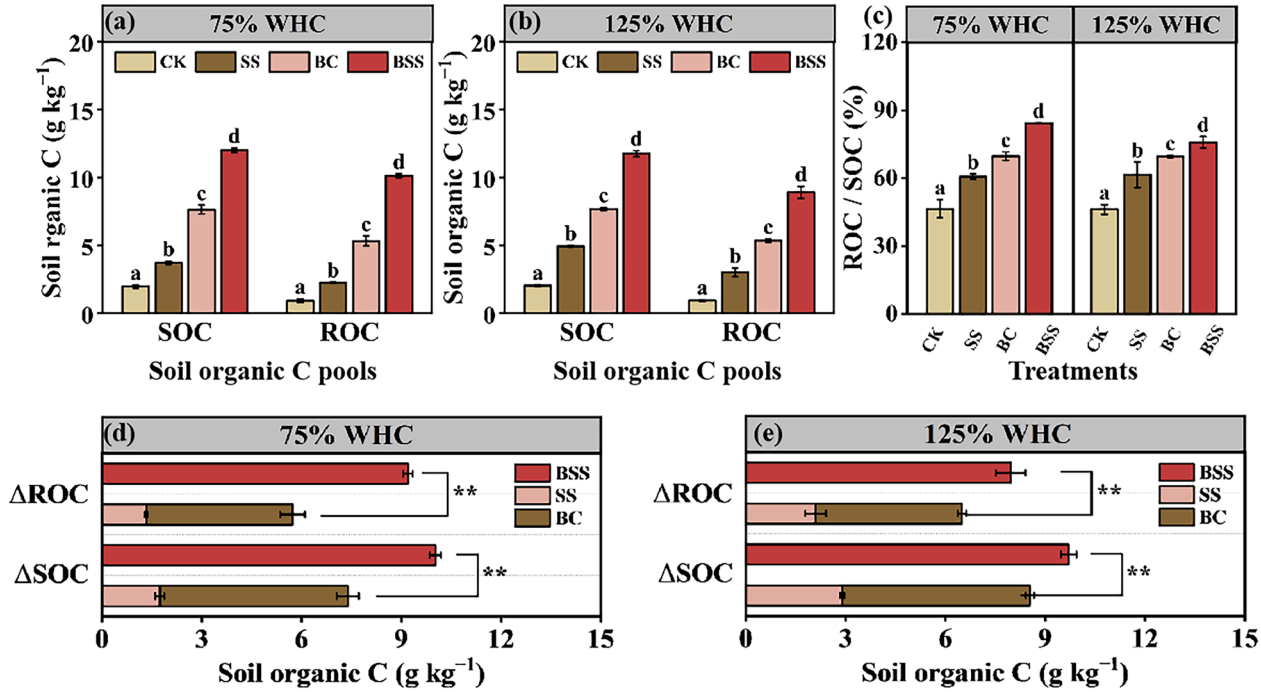


**Fig. 5** Changes in SOC and ROC, the ROC/SOC ratio, and ΔSOC and ΔROC. **a**, **b** SOC and ROC contents under 75% WHC and 125% WHC, respectively. **c** ROC/SOC ratio under 75% WHC and 125% WHC. **d**, **e** Increments in SOC and ROC relative to CK (ΔSOC and ΔROC) under 75% WHC and 125% WHC, respectively. CK, unamended soil (control); BC, soil + CBC; SS, soil + litter; and BSS, soil + CBC + litter. Different lowercase letters indicate significant differences among treatments within each moisture condition ($P < 0.05$). Asterisks indicate significant differences between BSS and the summed increments of BC and SS (*$P < 0.05$, **$P < 0.01$)

treatments, BNC was the primary contributor to ΔMNC in SS and BSS, whereas FNC contributed most to ΔMNC in BC (Fig. 4g, h).

### 3.5 Soil organic carbon (SOC) and recalcitrant organic C (ROC)

SOC and ROC and the ROC/SOC ratio are shown in Fig. 5. Under both moisture conditions, SOC and ROC contents were significantly higher in BSS than in CK, BC, and SS ($P < 0.05$; Fig. 5a, b). Specifically, SOC content in BSS increased by 491.86%, 55.09%, and 174.87% relative to CK, BC, and SS, respectively ($P < 0.05$; Fig. 5a, b), while ROC content increased by 922.63%, 78.36%, and 260.15%, respectively ($P < 0.05$; Fig. 5a, b). Compared with CK, SOC and ROC contents also increased significantly in SS ($P < 0.05$; Fig. 5a, b), with mean increases of 115.46% and 183.94%, respectively. The ROC/SOC ratio was significantly higher in BC, SS, and BSS than in CK, reaching 1.50-, 1.32-, and 1.73-fold that of CK, respectively ($P < 0.05$, Fig. 5c). To further evaluate treatment effects, we calculated the relative increments of SOC (ΔSOC) and ROC (ΔROC) using CK as the reference. ΔSOC and ΔROC in BSS exceeded the sums of those in BC and SS by 23.33% and 40.12%, respectively ($P < 0.05$; Fig. 5d, e).

### 3.6 Microbial community characteristics in the detritusphere

Microbial community composition and predicted functional profiles in detritusphere soil are presented in Fig. 6. At the phylum level, the bacterial community was dominated by Proteobacteria, Planctomycetes, and Gemmatimonadetes, which together accounted for more than 50% of the total relative abundance (Fig. 6a). Relative to SS, BSS increased the relative abundances of Proteobacteria and Firmicutes, two phyla commonly associated with copiotrophic or resource-responsive lifestyles, while reducing the relative abundance of Cyanobacteria. BSS also increased Acidobacteria, Chloroflexi, Gemmatimonadetes, and Nitrospirae, but decreased Planctomycetes and Euryarchaeota (Fig. 6a). Among the 12 carbon-cycling-related bacterial genera with relative abundances > 0.5%, BSS showed higher abundances of *Subgroup_10*, *Thiobacillus*, *Thioalkalispira*, and *Azoarcus*, but lower abundances of *Phormidium_MBIC10003* and *Rhodopirellula* compared with SS (Fig. 6b). PICRUSt2-based functional predictions indicated that, among the 20 most abundant KEGG level-2 categories, 19 showed higher predicted relative abundances in BSS than in SS, with Transcription being the only exception (Fig. 6c).

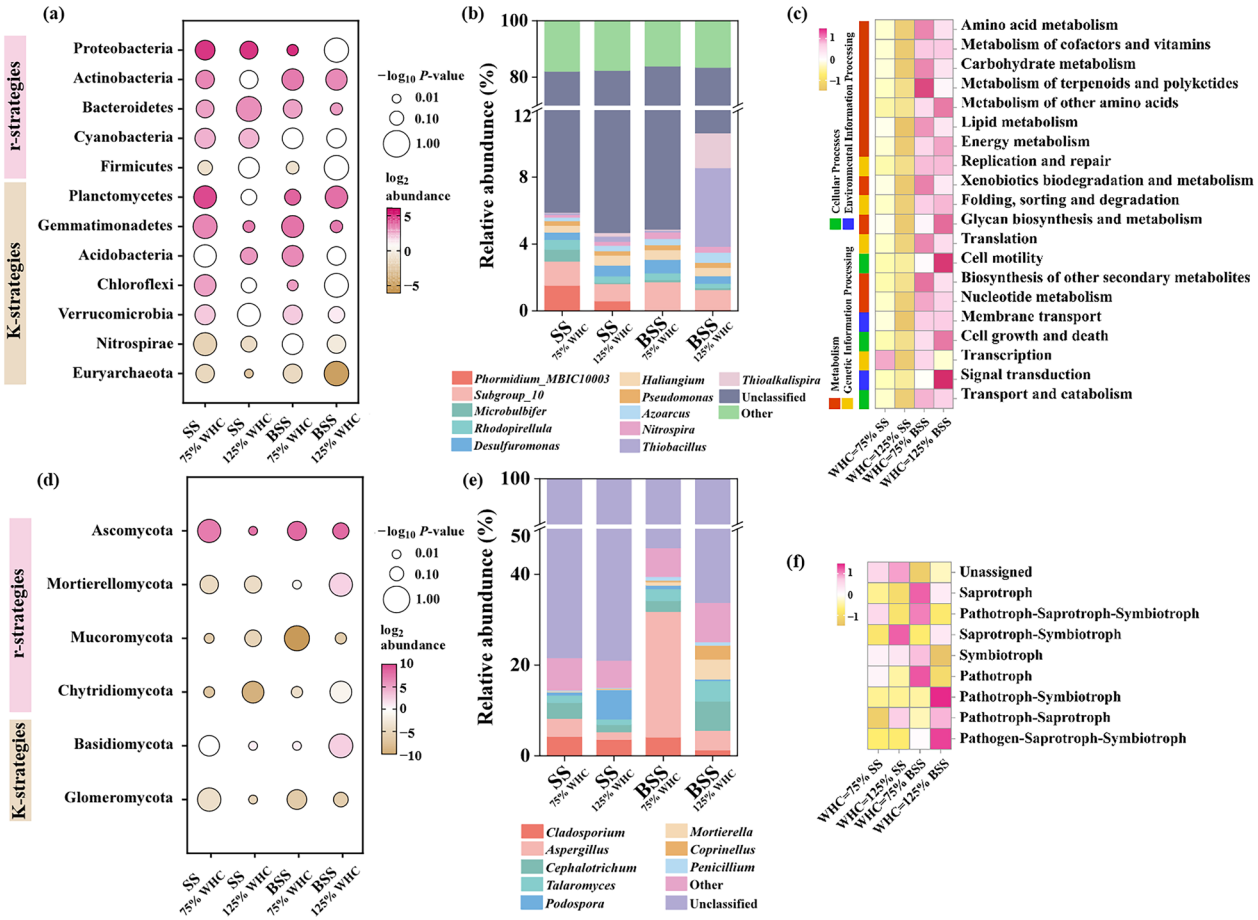


**Fig. 6** Changes in soil microbial community characteristics in detritusphere soils. **a**, **d** Bubble plots of carbon-cycling-related bacterial and fungal phyla. **b**, **e** Relative abundances of bacterial and fungal genera associated with carbon cycling. **c** Relative abundances of bacterial KEGG metabolic pathways predicted by PICRUSt2. **f** Relative abundances of fungal functional guilds predicted by FUNGuild. SS, soil + litter; and BSS, soil + CBC + litter. In bubble plots, color indicates the $\log_2$-transformed relative abundance at the phylum level, and bubble size represents statistical significance, expressed as $-\log_{10}(P)$. In functional prediction heatmaps, categories are ordered by decreasing mean relative abundance

At the fungal phylum level, Ascomycota was the dominant phylum, accounting for more than 60% of the total relative abundance (Fig. 6d). BSS increased the relative abundances of Ascomycota, Mortierellomycota, Chytridiomycota, and Basidiomycota relative to SS, but decreased those of Mucoromycota and Glomeromycota (Fig. 6d). Among eight carbon-cycling-related fungal genera with relative abundances > 0.5%, BSS showed higher relative abundances of *Aspergillus*, *Talaromyces*, *Mortierella*, and *Coprinellus*, but a lower relative abundance of *Penicillium* compared with SS (Fig. 6e). FUNGuild analysis further classified the fungal community into three broad trophic modes, namely saprotrophy, symbiotrophy, and pathotrophy, encompassing eight functional guilds. The relative abundance of the dominant saprotrophic guild was significantly higher in BSS than in SS, whereas no significant changes were observed for the other guilds (Fig. 6f; Fig. S2).

## 4 Discussion

### 4.1 CBC promotes litter decomposition and enhances lignin phenol accumulation in the detritusphere

Litter mass loss dynamics reflect the decomposition and transformation of plant-derived C (Ding et al. 2023). The litter mass loss rate was significantly higher during days 0–10 than thereafter ($P < 0.05$; Fig. 2a, b). CBC significantly affected mass loss in both the rapid and sustained phases, whereas moisture only influenced the rapid phase, and no CBC × moisture interaction was detected (Table S4). The consistently greater mass loss in BSS than in SS (Fig. 2a, b) indicates that CBC accelerated litter decomposition. Greater litter mass loss therefore reflects accelerated transformation of the residual litter pool, which may also enhance the transfer of litter-derived C to the surrounding detritusphere.

FTIR spectra provided evidence for enhanced lignin oxidation under CBC addition (Fig. 2c). Relative to SS

residues, BSS residues showed stronger bands at 3600–3300 $cm^{-1}$ (O–H), 1645 $cm^{-1}$ (aromatic C=C/carboxyl C=O), and 1515 $cm^{-1}$ (lignin aromatics), suggesting relative enrichment of oxygen-containing and aromatic structures (Fig. 2c) (Boeriu et al. 2004). This interpretation is supported by the higher (Ad/Al)v and (Ad/Al)s ratios in BSS than in SS ($P < 0.05$; Fig. 3d, e), which are established indicators of greater lignin oxidation (Thevenot et al. 2010). The enhanced bands at 1475 $cm^{-1}$ (C–H bending) and 1080 $cm^{-1}$ (C–O–C vibrations) in BSS further point to degradation and transformation of structural polysaccharides, yielding products of increased chemical complexity and stability (Xia et al. 2017). Importantly, the higher ROC/SOC ratio in BSS (Fig. 5c) is consistent with the accumulation of these relatively stable decomposition products. Collectively, these results suggest that CBC accelerated litter decomposition and promoted lignin oxidation, thereby facilitating the accumulation of lignin-derived products that contribute to SOC persistence in the detritusphere.

Cinnamyl, vanillyl, and syringyl lignin phenols are characteristic biomarkers of lignin oxidative degradation from plant residues and serve as molecular fingerprints for tracing the fate of plant-derived C in soil (Thevenot et al. 2010; Yang et al. 2022). PCA of lignin phenol composition showed that PC1 explained 67.76% of the total variation, with BSS clearly separated from SS along the positive PC1 axis (Fig. 7a; Table S4), indicating that CBC significantly altered lignin phenol composition in the detritusphere. Three-way ANOVA confirmed that litter input was the primary driver of lignin phenol variation ($P < 0.001$; Fig. 7b). Relative to SS, BSS significantly increased the contents of vanillyl phenols and total lignin phenols (Fig. 3a–c), and Spearman correlation showed that vanillyl phenols, total lignin phenols, and (Ad/Al)v were positively correlated with litter mass loss ($P < 0.05$; Fig. 7c). This coordinated response suggests that enhanced litter decomposition was accompanied by greater transfer of lignin-derived C from plant residues to the detritusphere. The resulting increase in soil lignin phenols therefore reflects intensified litter-derived C transformation and redistribution during decomposition (Thevenot et al. 2010; Vidal et al. 2021).

### 4.2 CBC reshapes detritusphere microbial communities to promote plant-C accumulation

The changes in lignin phenol accumulation and oxidation were associated with shifts in the detritusphere microbial community. Biochar can influence microbial taxa and enzyme activities involved in plant-derived organic matter transformation by regulating salt stress, nutrient supply, and micro-environmental conditions (Feng and Wang 2023). In the bacterial community, BSS enriched several taxa linked to organic matter turnover. Notably, the relative abundance of Bacteroidetes, a phylum with strong capacity for utilizing labile organic matter and plant cell-wall polysaccharides (Martin et al. 2025), was higher in BSS than in SS, and its abundance was positively correlated with the lignin oxidation index (Ad/Al)s ($P < 0.05$; Fig. 7d). Similarly, the sulfur-oxidizing chemolithoautotrophs *Thiobacillus* and *Thioalkalispira*, which can influence soil redox status and C fixation (Ghosh and Dam 2009), were enriched in BSS and positively correlated with vanillyl phenols, total lignin phenols, and (Ad/Al)s ($P < 0.05$; Fig. 7d). In the fungal community, BSS showed higher relative abundance of Basidiomycota, a phylum with known lignin-degrading potential (Taskin et al. 2019), and its abundance was significantly correlated with lignin phenol contents ($P < 0.05$; Fig. 7e). At the genus level, *Preussia*, *Talaromyces*, *Mortierella*, *Coprinellus*, and *Penicillium* were significantly correlated with litter mass loss and specific lignin monomers ($P < 0.05$; Fig. 7e), consistent with reported capacities to decompose cellulose, hemicellulose, and lignin (Li et al. 2023a; Sivaramanan 2014; Méndez-Líter et al. 2021). Overall, these patterns suggest that CBC promoted litter decomposition and plant-derived lignin phenol accumulation by enriching microbial taxa associated with lignocellulose degradation in the detritusphere.

It should be noted that litter bag incubation may have altered the micro-environmental conditions relative to natural field settings—for example, by modifying moisture retention, gas exchange, or substrate accessibility within the bags—and could thus have influenced decomposition rates to some extent (Kurz-Besson et al. 2005; Li et al. 2022). Nevertheless, the standardized litter preparation and incubation procedures enabled a robust comparison of relative treatment effects under controlled conditions. Importantly, the consistently greater litter mass loss and higher abundances of decomposition-associated taxa in BSS than in SS across both moisture regimes and all sampling times indicate that the positive effect of CBC on litter decomposition is a consistent treatment response, rather than an artifact of the incubation system. Therefore, while the absolute decomposition rates may not directly mirror those in undisturbed field soils, the relative treatment differences observed in this microcosm study provide meaningful insights into the mechanisms by which CBC enhances litter decomposition and plant-derived C accumulation in the detritusphere.

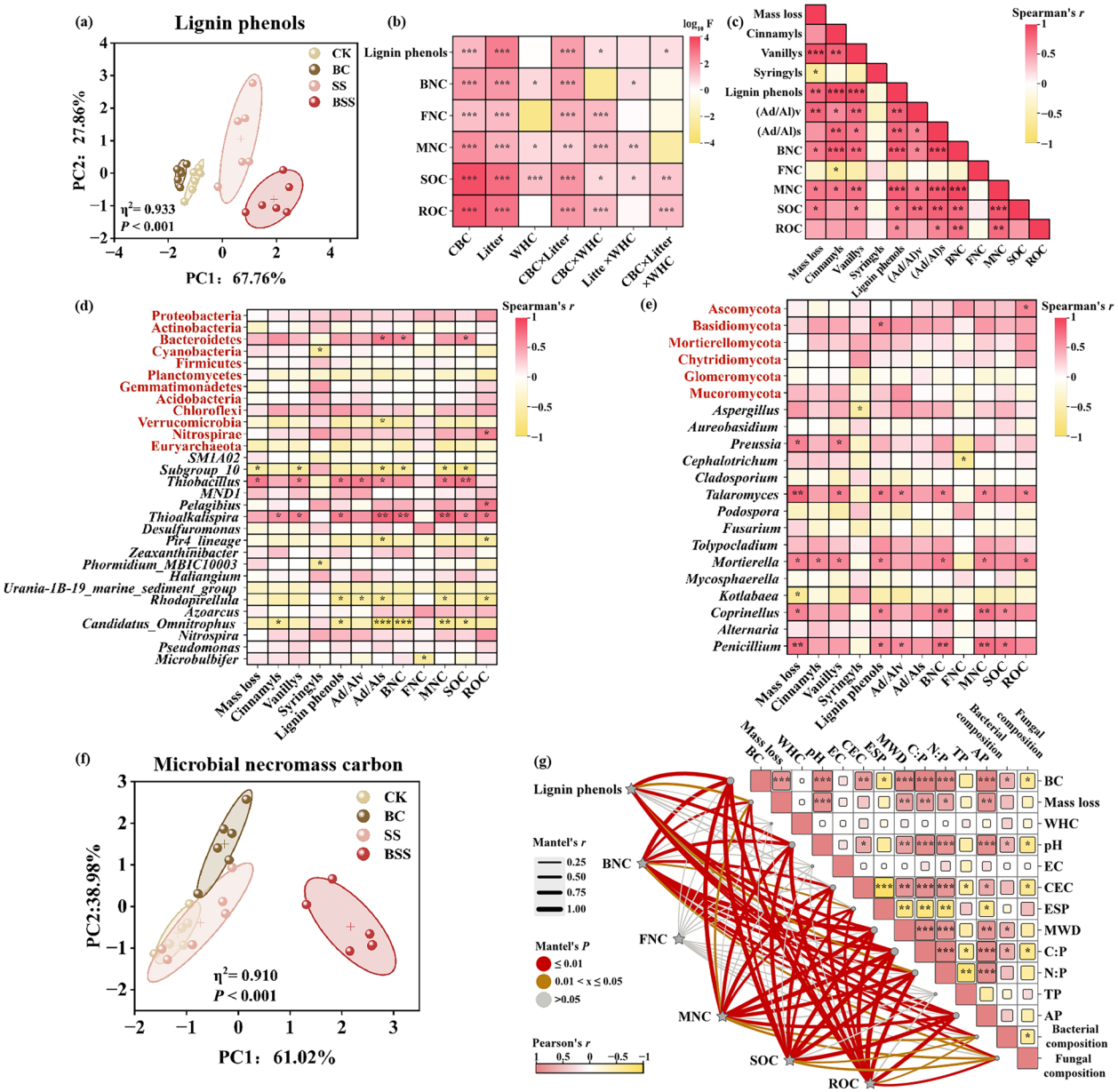


**Fig. 7** Driving factors of lignin phenols, MNC, and soil organic C fractions in coastal salt-affected soil. **a** PCA of lignin phenol monomer composition. **b** Heatmap of three-way ANOVA results showing the effects of CBC, litter addition, and WHC on lignin phenols, BNC, FNC, MNC, SOC, and ROC. **c** Spearman correlations among litter mass loss, cinnamyl, vanillyl, syringyl, total lignin phenols, (Ad/Al)v, (Ad/Al)s, BNC, FNC, MNC, SOC, and ROC. **d**, **e** Correlation heatmaps linking (**d**) bacterial and (**e**) fungal taxa (phylum and genus) with litter mass loss, lignin phenols, (Ad/Al)v, (Ad/Al)s, BNC, FNC, MNC, SOC, and ROC. **f** PCA of MNC composition. **g** Mantel tests linking lignin phenols, BNC, FNC, MNC, SOC, and ROC with CBC, litter mass loss, WHC, soil properties, and microbial community attributes. In panel (**g**), the color gradient denotes Pearson's *r*, line width denotes Mantel's *r*, and line color denotes Mantel test significance. **P* < 0.05, ***P* < 0.01, ****P* < 0.001

### 4.3 CBC and litter synergistically enhance microbial necromass C accumulation in the detritusphere

MNC is a key microbial-derived component of the SOC pool (Liang et al. 2017). Amino sugars, including MurA, GluN, and GalN, are widely used as biomarkers of microbial necromass, with MurA and GluN serving as proxies for bacterial (BNC) and fungal (FNC) necromass, respectively (Joergensen 2018). PCA of MNC composition showed that PC1 explained 61.02% of the total variance; CK and SS largely overlapped, whereas BC and BSS were clearly separated from CK, with BSS showing the greatest shift along the positive PC1 axis (Fig. 7f; Table S5).

This indicates that CBC markedly altered MNC composition, particularly when co-applied with litter. Among all treatments, BSS had the highest BNC and MNC contents ($P < 0.05$; Fig. 4d, e), and the increase in MNC relative to CK (ΔMNC) was primarily driven by ΔBNC in both SS and BSS (Fig. 4g, h). Notably, the increase in BNC (ΔBNC) under BSS exceeded the sum of the individual increases under BC and SS. Three-way ANOVA confirmed a significant CBC × litter interaction for BNC ($P < 0.05$; Fig. 7b), indicating a synergistic effect of CBC and litter on BNC accumulation in the BSS treatment.

The shift toward greater bacterial contribution to MNC was further supported by the lower GluN/MurA and higher BNC/MNC ratios in BSS (Fig. 4c, f). This pattern suggests that litter decomposition provided pulses of labile substrates that preferentially stimulated bacterial growth and turnover during the early and middle stages of incubation, generating abundant precursors for bacterial necromass formation while potentially constraining fungal necromass accumulation (Bai et al. 2024; Wang et al. 2024). Consistently, BNC was positively correlated with the relative abundance of Bacteroidetes and the genus *Thioalkalispira* ($P < 0.05$; Figs. 6b; 7d), taxa consistent with fast-growing, high-turnover strategies that may contribute to bacterial biomass production and turnover (Camenzind et al. 2023).

Biochar can alleviate microbial salinity-alkalinity stress by improving soil structure, reducing ESP, and increasing nutrient availability (Fig. 1), thereby shifting microbial energy allocation from maintenance toward growth and enhancing microbial C use efficiency, biomass, and turnover (Zhang et al. 2025a; Qiao et al. 2025). In this study, CBC increased soil EC (Fig. 1a), likely due to the release of soluble mineral ions (e.g., $K^+$, $Ca^{2+}$, $Mg^{2+}$, and $SO_4^{2-}$) from biochar, which may pose a short-term salinity risk in coastal salt-affected soils (Wang et al. 2024). However, the concurrent increases in CEC, SOC, TP, and AP, together with reduced ESP and improved aggregate stability, indicated that CBC generally improved soil quality and microbial habitat conditions (Fig. 1). Collectively, these improvements in the detritusphere microenvironment likely promoted the microbial transformation of litter-derived C and enhanced the accumulation of microbial-derived organic C.

### 4.4 CBC and litter synergistically promote SOC and ROC accumulation through coupled plant- and microbial-derived C stabilization

SOC content and stability are key determinants of soil health and C sequestration potential (Ma et al. 2023). Both plant-derived C (represented by lignin phenols) and MNC are major contributors to SOC, and the relatively resistant nature of ROC, typically enriched in alkyl and aromatic C, provides a useful indicator of the accumulation of relatively recalcitrant organic C (Suárez-Abelenda et al. 2014; Ramos et al. 2025). Both CBC and litter input increased SOC and ROC contents (Fig. 5a, b), and the increases in ΔSOC and ΔROC under BSS were significantly greater than the summed increases in SS and BC ($P < 0.05$; Fig. 5d, e). Three-way ANOVA results confirmed significant CBC × litter interactions for SOC and ROC ($P < 0.05$; Fig. 7a), supporting a synergistic effect of CBC and litter on SOC and ROC accumulation. Importantly, because biochar-derived C is only partially recovered by Walkley–Black oxidation (Knicker et al. 2007; Hardy and Dufey 2017), the increase in ROC should not be attributed solely to direct biochar-C input, but rather to the combined effects of exogenous C and the synergistically enhanced formation and retention of oxidation-resistant C fractions. This is consistent with the increased accumulation of total lignin phenols and BNC in BSS (Figs. 3a, b; 4c, d), suggesting that the co-application of CBC and litter promoted the coupled accumulation of plant- and microbial-derived organic C in the detritusphere. Biochar-enhanced litter decomposition increased overall litter mass loss, but the decomposition of individual litter components was likely non-uniform. During litter decay, relatively labile components, including soluble carbohydrates, cellulose, and hemicellulose, are preferentially decomposed and mineralized, with part of this C ultimately released as $CO_2$, whereas lignin, as a relatively recalcitrant aromatic biopolymer, generally decomposes more slowly (Wang et al. 2022). Lignin can subsequently be depolymerized by extracellular oxidative enzymes into lower-molecular-weight lignin-derived phenolic and aromatic intermediates (Janusz et al. 2017). These intermediates may be retained in the detritusphere through sorption to biochar and soil mineral surfaces and physical occlusion within aggregates, thereby reducing their accessibility to further microbial degradation and favoring the relative enrichment and persistence of plant-derived C despite greater overall litter mass loss (Feng et al. 2021; Huang et al. 2019; Wang et al. 2014).

The stabilization of these accumulated C fractions was likely reinforced by mineral-organic associations including adsorption, ligand exchange, inner-sphere complexation, cation bridging, co-precipitation, and aggregate occlusion (Qiao et al. 2025). Relative to SS, BSS significantly increased the contents of organic C associated with reducible Fe phases ($DOC_{Na_2S_2O_4}$) and non-reducible organo-metal/mineral complexes ($DOC_{Na_4P_2O_7}$) by 50.44% and 23.87%, respectively ($P < 0.05$; Fig. S2). These fractions were positively correlated with SOC, ROC, lignin phenols, BNC, and MNC ($P < 0.05$; Fig. S5), indicating that mineral association contributed to the

retention of both plant- and microbial-derived C. Given that mineral association reduces organic C desorbability and its accessibility to microorganisms and extracellular enzymes (Hemingway et al. 2019; Huang et al. 2020), CBC likely enhanced SOC stabilization by promoting mineral-organic associations. In addition, the porous structure and surface functional groups of CBC (Fig. S1; Luo et al. 2024) may further protect organic compounds through pore entrapment, surface adsorption, and hydrophobic interactions (He et al. 2017; Qiu et al. 2021; Weng et al. 2022; Qiu et al. 2022; Zhao and Zhou 2019). In coastal salt-affected soils of the Yellow River Delta, reactive minerals such as Fe phosphates, aluminosilicates, and Fe silicates can deposit on biochar surfaces (Zheng et al. 2018b), providing additional interfaces for mineral-organic association formation.

Mantel tests further revealed that CBC, litter decomposition, soil properties, and microbial community structure (represented by the first PCoA axis) were jointly associated with variations in lignin phenols, MNC, SOC, and ROC ($P < 0.05$; Fig. 7g). Compared with SS, BSS had higher CEC, MWD, and AP, lower ESP, and a C:N:P ratio (Fig. 1) closer to the average microbial biomass stoichiometry of 60:7:1 (Cleveland and Liptzin 2007). These changes suggest that CBC improved the salt-affected soil environment, and promoted microbial community shifts favorable for C transformation (Fig. 6). As a microbial C hotspot, the detritusphere receives labile C from decomposing litter, stimulating microbial growth and turnover and accelerating necromass accumulation (Feng and Wang 2023; Tan et al. 2025). Thus, CBC may couple accelerated litter turnover with enhanced physicochemical retention of lignin-derived C, while stimulating microbial turnover and necromass accumulation, thereby supporting the coupled accumulation of plant- and microbial-derived C in coastal salt-affected soils.

## 5 Conclusion

This study demonstrates that co-application of CBC and *Suaeda salsa* litter synergistically increased lignin phenols and BNC in the detritusphere, concurrently enhancing SOC, ROC, and mineral-associated organic C pools. Litter input was the primary driver of lignin phenol accumulation, whereas CBC was the dominant factor controlling litter decomposition, MNC, SOC, and ROC. Mechanistically, CBC and litter appeared to act through complementary pathways. Litter input continuously supplied plant-derived biochemical substrates to

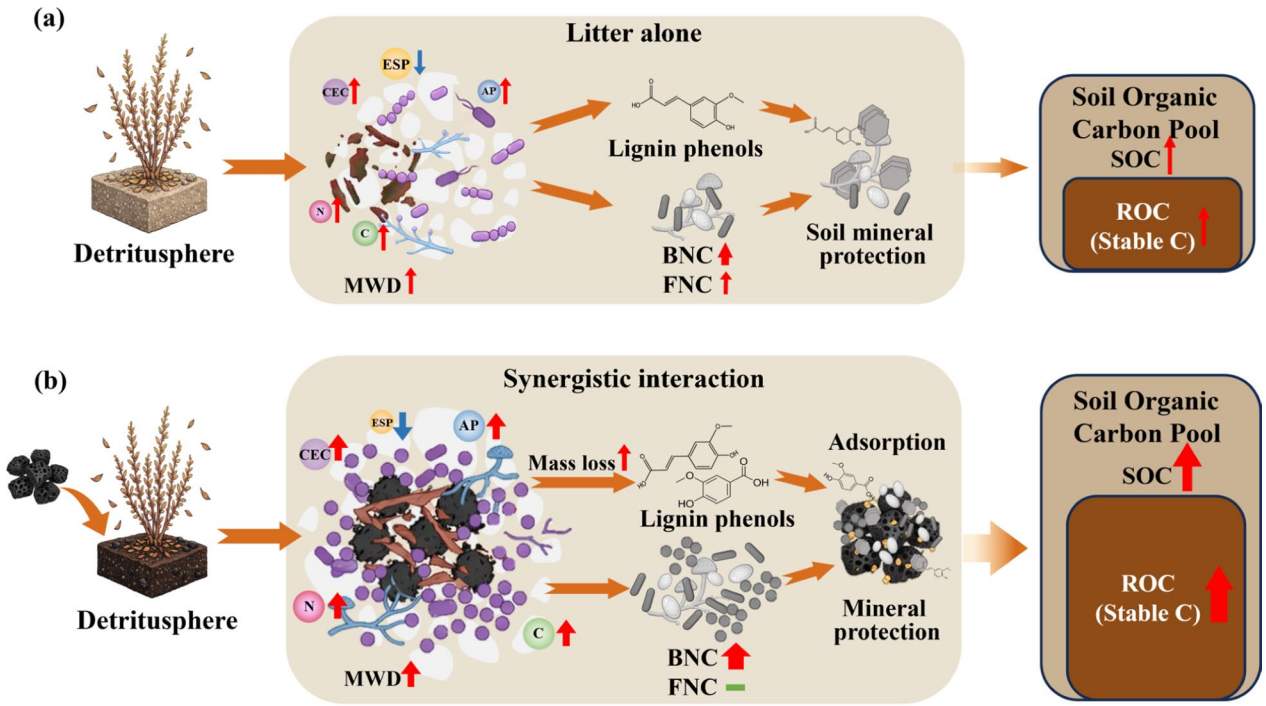


**Fig. 8** Schematic diagram illustrating the mechanisms by which biochar promotes the accumulation and stabilization of lignin phenols and MNC in the *Suaeda salsa* detritusphere in coastal salt-affected soil. **a** Litter input promotes the accumulation of lignin phenols, BNC, and FNC in the detritusphere, and enhances organic C stabilization through mineral association, thereby increasing the organic C pool and its stability in coastal salt-affected soil. **b** Biochar input increases lignin phenol and BNC accumulation by regulating microbial interactions, promoting litter decomposition, and facilitating C transformation in the detritusphere. Meanwhile, its porous structure, surface functional groups, and mineral components strengthen the physical protection and mineral association of organic C, thereby enhancing the stability of the organic C pool

the detritusphere, whereas CBC addition was associated with enhanced accumulation and retention of plant- and microbial-derived organic C, potentially through: (1) alleviation of salinity–alkalinity stress and improvements in soil structure and nutrient availability; (2) shifts in the detritusphere microbial community toward taxa associated with litter decomposition and necromass accumulation; and (3) physicochemical protection via pore entrapment, surface adsorption, and mineral–organic associations. Together, these processes were associated with enhanced SOC accumulation and stability in the salt-affected detritusphere (Fig. 8). This study provides mechanistic insights into biochar-mediated C transformation and stabilization in coastal salt-affected detritusphere soils. However, C dynamics in natural coastal wetlands are influenced by multiple interacting factors, including tidal flooding, root activity, seasonal temperature changes, and long-term redox fluctuations. Future work should verify the long-term effects of biochar and litter inputs on detritusphere C fate through field trials and in situ decomposition experiments, ideally combined with stable isotope labeling to trace the transformation and partitioning of plant- and microbial-derived C into stable SOC pools.

## Supplementary Information

The online version contains supplementary material available at https://doi.org/10.1007/s42773-026-00660-6.

Supplementary material 1.

**Funding**

This study was funded by the National Natural Science Foundation of China (42477243), the Key Research and Development Program of Shandong Province, China (2022SFGC0302), Natural Science Foundation of Shandong Province (ZR2026ZD10), and Shandong Province National Talents Supporting Program (2023GJJLJRC-059).

**Author contributions**

Xianxiang Luo: Project administration, resources, validation, conceptualization, funding acquisition, writing—review and editing, supervision. Zhimeng Liang: Investigation, data curation, formal analysis, writing—original draft. Liuqingqing Liu: Investigation, validation, writing-review and editing. Kun Chen: Formal analysis, visualization. Lize Zhao: Investigation, formal analysis, visualization. Qiang Liu: Formal analysis, visualization. Zhengyang Wang: Investigation, validation. Yufei Cao: Investigation, validation. Fengmin Li: Resources, validation. Hao Zheng: Conceptualization, resources, visualization, writing—review and editing. All authors read and approved the final manuscript.

**Data availability**

The 16S and ITS metabarcoding data generated in this study have been deposited in the NCBI Sequence Read Archive (SRA) under BioProject accession number PRJNA1481187. All other data generated or analyzed during this study are available from the corresponding author upon reasonable request.

## Declarations

**Competing interests**

The authors declare that they have no known competing financial interests or personal relationships that could have appeared to influence the work reported in this paper.

**Author details**

[1]Institute of Coastal Environmental Pollution Control, Ministry of Education Key Laboratory of Marine Environment and Ecology, Frontiers Science Center for Deep Ocean Multispheres and Earth System, Ocean University of China, Qingdao 266100, China. [2]Qingdao Engineering Research Center of Land-Ocean Integration for Emerging Pollutant Control and Ecological Restoration, Qingdao 266100, China. [3]College of Life Sciences, Shihezi University, Shihezi 832000, China.

Received: 7 February 2026 Revised: 3 September 2026 Accepted: 23 September 2026
Published online: 29 October 2026

**References**

Bai X, Zhai G, Yan Z, An S, Liu J, Huo L, Dippold MA, Kuzyakov Y (2024) Effects of microbial groups on soil organic carbon accrual and mineralization during high- and low-quality litter decomposition. CATENA 241:108051. https://doi.org/10.1016/j.catena.2024.108051

Benslama A, Benbrahim F, Rym-Gadoum L, Gómez-Lucas I, Mordan-Vidal MM, Navarro-Pedreño J, Bech-Borrás J (2024) Soil carbon storage under different types of arid land use in Algeria. Environ Geochem Health 46:330. https://doi.org/10.1007/s10653-024-02036-w

Boeriu CG, Bravo D, Gosselink RJA, van Dam JEG (2004) Characterisation of structure-dependent functional properties of lignin with infrared spectroscopy. Ind Crops Prod 20:205–218. https://doi.org/10.1016/j.indcrop.2004.04.022

Camenzind T, Mason-Jones K, Mansour I, Rillig MC, Lehmann J (2023) Formation of necromass-derived soil organic carbon determined by microbial death pathways. Nat Geosci 16:115–122. https://doi.org/10.1038/s41561-022-01100-3

Chen H, Zhao G, Li Y, Wang D, Ma Y (2019) Monitoring the seasonal dynamics of soil salinization in the Yellow River delta of China using Landsat data. Nat Hazards Earth Syst Sci 19:1499–1508. https://doi.org/10.5194/nhess-19-1499-2019

Chen J, Wang H, Hu G, Li X, Dong Y, Zhuge Y, He H, Zhang X (2021) Distinct accumulation of bacterial and fungal residues along a salinity gradient in coastal salt-affected soils. Soil Biol Biochem 158:108266. https://doi.org/10.1016/j.soilbio.2021.108266

Chen Z, He L, Ma J, Ma J, Ye J, Yu Q, Zou P, Sun W, Lin H, Wang F, Zhao X, Wang Q (2024) Long-term successive biochar application increases plant lignin and microbial necromass accumulation but decreases their contributions to soil organic carbon in rice-wheat cropping system. Glob Change Biol Bioenergy 16(6):e13137. https://doi.org/10.1111/gcbb.13137

Cheng Z, Guo J, Jin W, Liu Z, Wang Q, Zha L, Zhou Z, Meng Y (2024) Responses of SOC, labile SOC fractions, and amino sugars to different organic amendments in a coastal saline-alkali soil. Soil Tillage Res 239:106051. https://doi.org/10.1016/j.still.2024.106051

Cleveland CC, Liptzin D (2007) C:N:P stoichiometry in soil: is there a "Redfield ratio" for the microbial biomass? Biogeochemistry 85:235–252. https://doi.org/10.1007/s10533-007-9132-0

Cui J, Ge T, Kuzyakov Y, Nie M, Fang C, Tang B, Zhou C (2017) Interactions between biochar and litter priming: a three-source $^{14}C$ and $\delta^{13}C$ partitioning study. Soil Biol Biochem 104:49–58. https://doi.org/10.1016/j.soilbio.2016.10.014

Ding Y, Wang D, Zhao G, Chen S, Sun T, Sun H, Wu C, Li Y, Yu Z, Li Y, Chen Z (2023) The contribution of wetland plant litter to soil carbon pool: decomposition rates and priming effects. Environ Res 224:115575. https://doi.org/10.1016/j.envres.2023.115575

Elias DMO, Mason KE, Goodall T, Taylor A, Zhao P, Otero-Fariña A, Chen H, Peacock CL, Ostle NJ, Griffiths R, Chapman PJ, Holden J, Banwart S, McNamara NP, Whitaker J (2024) Microbial and mineral interactions decouple

litter quality from soil organic matter formation. Nat Commun 15:10063. https://doi.org/10.1038/s41467-024-54446-0
Feng X, Wang S (2023) Plant influences on soil microbial carbon pump efficiency. Glob Change Biol 29:3854–3856. https://doi.org/10.1111/gcb.16728
Feng D, Guo D, Zhang Y, Sun S, Zhao Y, Shang Q, Sun H, Wu J, Tan H (2021) Functionalized construction of biochar with hierarchical pore structures and surface O-/N-containing groups for phenol adsorption. Chem Eng J 410:127707. https://doi.org/10.1016/j.cej.2020.127707
Ghosh W, Dam B (2009) Biochemistry and molecular biology of lithotrophic sulfur oxidation by taxonomically and ecologically diverse bacteria and archaea. FEMS Microbiol Rev 33:999–1043. https://doi.org/10.1111/j.1574-6976.2009.00187.x
Hardy B, Dufey J (2017) The resistance of centennial soil charcoal to the "Walkley-Black" oxidation. Geoderma 303:37–43. https://doi.org/10.1016/j.geoderma.2017.05.001
He P, Yu Q, Zhang H, Shao L, Lü F (2017) Removal of copper (II) by biochar mediated by dissolved organic matter. Sci Rep 7:7091. https://doi.org/10.1038/s41598-017-07507-y
Hemingway JD, Rothman DH, Grant KE, Rosengard SZ, Eglinton TI, Derry LA, Galy VV (2019) Mineral protection regulates long-term global preservation of natural organic carbon. Nature 570(7760):228–231. https://doi.org/10.1038/s41586-019-1280-6
Hu D, Zhu G, Wu P, Zhang S, Cheng D (2026) High-quality litter drives a stronger home-field advantage of leaf decomposition in young plantations. Funct Ecol 40(1):97–112. https://doi.org/10.1111/1365-2435.70219
Huang W, Hammel KE, Hao J, Thompson A, Timokhin VI, Hall SJ (2019) Enrichment of lignin-derived carbon in mineral-associated soil organic matter. Environ Sci Technol 53(13):7522–7531. https://doi.org/10.1021/acs.est.9b01834
Huang W, Ye C, Hockaday WC, Hall SJ (2020) Trade-offs in soil carbon protection mechanisms under aerobic and anaerobic conditions. Glob Change Biol 26(6):3726–3737. https://doi.org/10.1111/gcb.15100
Janusz G, Pawlik A, Sulej J, Świderska-Burek U, Jarosz-Wilkołazka A, Paszczyński A (2017) Lignin degradation: microorganisms, enzymes involved, genomes analysis and evolution. FEMS Microbiol Rev 41(6):941–962. https://doi.org/10.1093/femsre/fux049
Joergensen RG (2018) Amino sugars as specific indices for fungal and bacterial residues in soil. Biol Fertil Soils 54:559–568. https://doi.org/10.1007/s00374-018-1288-3
Knicker H, Müller P, Hilscher A (2007) How useful is chemical oxidation with dichromate for the determination of "black carbon" in fire-affected soils? Geoderma 142:178–196. https://doi.org/10.1016/j.geoderma.2007.08.010
Kurz-Besson C, Coûteaux MM, Thiéry JM, Berg B, Remacle J (2005) A comparison of litterbag and direct observation methods of Scots pine needle decomposition measurement. Soil Biol Biochem 37(12):2315–2318. https://doi.org/10.1016/j.soilbio.2005.03.022
Kuzyakov Y, Blagodatskaya E (2015) Microbial hotspots and hot moments in soil: concept & review. Soil Biol Biochem 83:184–199. https://doi.org/10.1016/j.soilbio.2015.01.025
Lehmann J, Cowie A, Masiello CA, Kammann C, Woolf D, Amonette JE, Cayuela ML, Camps-Arbestain M, Whitman T (2021) Biochar in climate change mitigation. Nature Geoscience 14:883–892. https://doi.org/10.1038/s41561-021-00852-8
Li X, Zheng X, Zhou Q, McNulty S, King JS (2022) Measurements of fine root decomposition rate: method matters. Soil Biol Biochem 164:108482. https://doi.org/10.1016/j.soilbio.2021.108482
Li F, Chen L, Zhao Z, Li Y, Yu H, Wang Y, Zhang J, Han Y (2023a) The changes of chemical molecular components in soil organic matter are associated with fungus *Mortierella capitata K*. Soil Tillage Res 227:105598. https://doi.org/10.1016/j.still.2022.105598
Li Q, Song Z, Xia S, Kuzyakov Y, Yu C, Fang Y, Chen J, Wang Y, Shi Y, Luo Y, Li Y, Chen J, Wang W, Zhang J, Fu X, Vancov T, Van Zwieten L, Liu C, Wang H (2023b) Microbial necromass, lignin, and glycoproteins for determining and optimizing blue carbon formation. Environ Sci Technol 58:468–479. https://doi.org/10.1021/acs.est.3c08229
Li Y, Zhang W, Li J, Zhou F, Liang X, Zhu X, He H, Zhang X (2023c) Complementation between microbial necromass and plant debris governs the long-term build-up of the soil organic carbon pool in conservation agriculture. Soil Biol Biochem 178:108963. https://doi.org/10.1016/j.soilbio.2023.108963
Liang C, Schimel JP, Jastrow JD (2017) The importance of anabolism in microbial control over soil carbon storage. Nat Microbiol 2:17105. https://doi.org/10.1038/nmicrobiol.2017.105
Liu Q, Meki K, Zheng H, Yuan Y, Shao M, Luo X, Li X, Jiang Z, Li F, Xing B (2023) Biochar application in remediating salt-affected soil to achieve carbon neutrality and abate climate change. Biochar 5:45. https://doi.org/10.1007/s42773-023-00244-8
Liu X, Tang S, Tou C, Chen J, Wanek W, Kuzyakov Y, Chadwick DR, Jones DL, Wu L, Ma Q (2025) Opposite roles of plant quality and soil exoenzymes in regulation of litter carbon transfer to fungal and bacterial necromass. Soil Biol Biochem 210:109940. https://doi.org/10.1016/j.soilbio.2025.109940
Luo X, Chen W, Liu Q, Wang X, Miao J, Liu L, Zheng H, Liu R, Li F (2024) Corn straw biochar addition elevated phosphorus availability in a coastal salt-affected soil under the conditions of different halophyte litter input and moisture contents. Sci Total Environ 908:168355. https://doi.org/10.1016/j.scitotenv.2023.168355
Ma T, Dai G, Zhu S, Chen D, Chen L, Lü X, Wang X, Zhu J, Zhang Y, He J, Bai Y, Han X, Feng X (2020) Vertical variations in plant- and microbial-derived carbon components in grassland soils. Plant Soil 446:441–455. https://doi.org/10.1007/s11104-019-04371-9
Ma Y, Woolf D, Fan M, Qiao L, Li R, Lehmann J (2023) Global crop production increase by soil organic carbon. Nat Geosci 16:1159–1165. https://doi.org/10.1038/s41561-023-01302-3
Macreadie PI, Costa MDP, Atwood TB, Friess DA, Kelleway JJ, Kennedy H, Lovelock CE, Serrano O, Duarte CM (2021) Blue carbon as a natural climate solution. Nat Rev Earth Environ 2:826–839. https://doi.org/10.1038/s43017-021-00224-1
Martin H, Rogers LA, Moushtaq L, Brindley AA, Forbes P, Quinton AR, Murphy ARJ, Hipperson H, Daniell TJ, Ndeh D, Amsbury S, Hitchcock A, Lidbury IDEA (2025) Metabolism of hemicelluloses by root-associated Bacteroidota species. ISME J 19(1):wraf022. https://doi.org/10.1093/ismejo/wraf022
Méndez-Líter J, de Eugenio LI, Nieto-Domínguez M, Prieto A, Martínez MJ (2021) *Hemicellulases* from Penicillium and *Talaromyces* for lignocellulosic biomass valorization: A review. Bioresour Technol 324:124623. https://doi.org/10.1016/j.biortech.2020.124623
Meng D, Zhang K, Liu Z, Zang Y, Liu S, Yang J, Bai E (2025) Refining amino sugar-based conversion factors for quantification of microbial necromass carbon in soils. Glob Change Biol 31:e70443. https://doi.org/10.1111/gcb.70443
Minamino Y, Fujitake N, Suzuki T, Yoshitake S, Koizumi H, Tomotsune M (2019) Effect of biochar addition on leaf-litter decomposition at soil surface during three years in a warm-temperate secondary deciduous forest, Japan. Sci Rep 9(1):16961. https://doi.org/10.1038/s41598-019-53615-2
Negacz K, Malek Ž, de Vos A, Vellinga P (2022) Saline soils worldwide: identifying the most promising areas for saline agriculture. J Arid Environ 203:104775. https://doi.org/10.1016/j.jaridenv.2022.104775
Nelson DW, Sommers LE (1996) Total carbon, organic carbon, and organic matter. In: Sparks D, Page A, Helmke P, Loeppert R, Soltanpour P, Tabatabai M, Johnston C, Sumner M (eds) Methods of soil analysis. Part 3. Chemical methods. Soil Science Society of America and American Society of Agronomy, Madison, pp 961-1010
Qiao L, Wang J, Wei S, Ren Y, Lichtfouse E, Han J (2025) The soil microbial carbon pump for carbon sequestration. Environ Chem Lett 23:1145–1151. https://doi.org/10.1007/s10311-025-01861-4
Qiu L, Wu J, Qian Y, Nafees M, Zhang J, Du W, Yin Y, Guo H (2021) Impact of biochar-induced vertical mobilization of dissolved organic matter, sulfamethazine and antibiotic resistance genes variation in a soil-plant system. J Hazard Mater 417:126022. https://doi.org/10.1016/j.jhazmat.2021.126022
Qiu M, Liu L, Ling Q, Cai Y, Yu S, Wang S, Fu D, Bao Hu, Wang X (2022) Biochar for the removal of contaminants from soil and water: a review. Biochar 4:19. https://doi.org/10.1007/s42773-022-00146-1
Qu W, Han G, Wang J, Li J, Zhao M, He W, Li X, Wei S (2021) Short-term effects of soil moisture on soil organic carbon decomposition in a coastal wetland of the Yellow River Delta. Hydrobiologia 848:3259–3271. https://doi.org/10.1007/s10750-020-04422-8
Rabbi SMF, Wilson BR, Lockwood PV, Daniel H, Young IM (2014) Soil organic carbon mineralization rates in aggregates under contrasting land uses. Geoderma 216:10–18. https://doi.org/10.1016/j.geoderma.2013.10.023

Ramos C, Zagal E, Timmusk S, Dube F, Paulino L, Ortiz J, Intriago-Ávila J, Fuentes JP (2025) Soil carbon sequestration in *Nothofagus obliqua* forests with different canopy cover levels under silvopastoral management. Agronomy 15:855. https://doi.org/10.3390/agronomy15040855

Shao P, Han H, Sun J, Yang H, Xie H (2022) Salinity effects on microbial derived-C of coastal wetland soils in the Yellow River Delta. Front Ecol Evol 10:872816. https://doi.org/10.3389/fevo.2022.872816

Sivaramanan S (2014) Isolation of cellulolytic fungi and their degradation on cellulosic agricultural wastes. JAIR 2:458–463. https://doi.org/10.13140/2.1.3633.4080

Su Z, Zhu X, Wang Y, Mao S, Shangguan Z (2022) Litter C and N losses at different decomposition stages of *Robinia pseudoacacia*: the weaker effects of soil enzyme activities compared with those of litter quality and the soil environment. Front Environ Sci 10:956309. https://doi.org/10.3389/fenvs.2022.956309

Suárez-Abelenda M, Kaal J, Camps Arbestain M, Knicker H, Macias-Vázquez IF (2014) Molecular characteristics of permanganate- and dichromate-oxidation-resistant soil organic matter from a black-C-rich colluvial soil. Soil Res 52:164–179. https://doi.org/10.1071/SR13195

Sun Z, Mou X, Tian H, Song H, Jiang H, Zhao J, Sun W, Sun W (2013) Phosphorus biological cycle in the different *Suaeda salsa* marshes of the Yellow River estuary, China. Environ Earth Sci 69:2595–2608. https://doi.org/10.1007/s12665-012-2081-5

Tan J, Huang J, Quan W, Su L, Liu Y, Cai Y, Li S, Guo P, Luo M (2025) Divergence of microbial carbon use efficiency and soil organic carbon along a tidal flooding gradient in a subtropical coastal wetland. Water Res 280:123527. https://doi.org/10.1016/j.watres.2025.123527

Tang Z, Wang D, Tian X, Bi X, Zhou Z, Luo F, Ning R, Li J (2024) Exploring the factors influencing the carbon sink function of coastal wetlands in the Yellow River Delta. Sci Rep 14:28938. https://doi.org/10.1038/s41598-024-80186-8

Taskin E, Branà MT, Altomare C, Loffredo E (2019) Biochar and hydrochar from waste biomass promote the growth and enzyme activity of soil-resident ligninolytic fungi. Heliyon 5:e02051. https://doi.org/10.1016/j.heliyon.2019.e02051

Thevenot M, Dignac MF, Rumpel C (2010) Fate of lignins in soils: a review. Soil Biol Biochem 42:1200–1211. https://doi.org/10.1016/j.soilbio.2010.03.017

Vannini A, Carbognani M, Chiari G, Forte TGW, Rodolfi M, Ganino T, Petraglia A (2023) Biochar effects on early decomposition of standard litter in a European beech forest (northern Italy). Sci Total Environ 903:166224. https://doi.org/10.1016/j.scitotenv.2023.166224

Vidal A, Klöffel T, Guigue J, Angst G, Steffens M, Hoeschen C, Mueller CW (2021) Visualizing the transfer of organic matter from decaying plant residues to soil mineral surfaces controlled by microorganisms. Soil Biol Biochem 160:108347. https://doi.org/10.1016/j.soilbio.2021.108347

Wang X, Cammeraat ELH, Cerli C, Kalbitz K (2014) Soil aggregation and the stabilization of organic carbon as affected by erosion and deposition. Soil Biol Biochem 72:55–65. https://doi.org/10.1016/j.soilbio.2014.01.018

Wang L, Zhou Y, Chen Y, Xu Z, Zhang J, Liu Y, Joly FX (2022) Litter diversity accelerates labile carbon but slows recalcitrant carbon decomposition. Soil Biol Biochem 168:108632. https://doi.org/10.1016/j.soilbio.2022.108632

Wang F, Liu J, Qin G, Zhang J, Zhou J, Wu J, Zhang L, Thapa P, Sanders CJR, Santos IR, Li X, Lin G, Weng Q, Tang J, Jiao N, Ren H (2023) Coastal blue carbon in China as a nature-based solution toward carbon neutrality. Innovation 4:100481. https://doi.org/10.1016/j.xinn.2023.100481

Wang X, Ding J, Han L, Tan J, Ge X, Nan Q (2024) Biochar addition reduces salinity in salt-affected soils with no impact on soil pH: a meta-analysis. Geoderma 443:116845. https://doi.org/10.1016/j.geoderma.2024.116845

Wang Y, Gao Y, Zheng H, Wang R, Ge Z, Miao Z (2025a) Biochar enhances soil organic carbon by stabilizing microbial necromass carbon in saline-alkaline topsoil. Agronomy 15:2472. https://doi.org/10.3390/agronomy15112472

Wang Y, Yan Y, Lu S, Li X, Wang N, Qi G, Lu H, Zhang Y, Li Y, Wang H, Liu H (2025b) Influence of biochar application on the residual carbon of soil microorganisms in the Yellow River Delta. Sci Soil Water Conserv 24(2):175–185. https://doi.org/10.16843/j.sswc.2025181

Weng Z, Van Zwieten L, Tavakkoli E, Rose MT, Singh BP, Joseph S, Macdonald LM, Kimber S, Morris S, Rose TJ, Archanjo BS, Tang C, Franks AC, Diao H, Schweizer S, Tobin MJ, Klein AR, Vongsvivut J, Chang SLY, Kopittke PM, Cowie A (2022) Microspectroscopic visualization of how biochar lifts the soil organic carbon ceiling. Nat Commun 13:5177. https://doi.org/10.1038/s41467-022-32819-7

Witzgall K, Vidal A, Schubert DI, Höschen C, Schweizer SA, Buegger F, Pouteau V, Chenu C, Mueller CW (2021) Particulate organic matter as a functional soil component for persistent soil organic carbon. Nat Commun 12(1):4115. https://doi.org/10.1038/s41467-021-24192-8

Xia M, Talhelm AF, Pregitzer KS (2017) Chronic nitrogen deposition influences the chemical dynamics of leaf litter and fine roots during decomposition. Soil Biol Biochem 112:24–34. https://doi.org/10.1016/j.soilbio.2017.04.011

Xie Z, Yu Z, Li Y, Wang G, Liu X, Tang C, Lian T, Adams J, Liu J, Liu J, Herbert SJ, Jin J (2022) Soil microbial metabolism on carbon and nitrogen transformation links the crop-residue contribution to soil organic carbon. Npj Biofilms Microbiomes 8(1):14. https://doi.org/10.1038/s41522-022-00277-0

Yan Y, Yin L, Li R, Deng B, Yang Q, Chen L, Zhang Z, Wang S, Zhang W (2026) How does wollastonite addition influence litter decomposition in a subtropical forest? The role of litter quality and soil fauna. Soil Biol Biochem 219:110174. https://doi.org/10.1016/j.soilbio.2026.110174

Yang W, Ding H, Puglia D, Kenny JM, Liu T, Guo J, Wang Q, Ou R, Xu P, Ma P, Lemstra PJ (2022) Bio-renewable polymers based on lignin-derived phenol monomers: synthesis, applications, and perspectives. SusMat 2:535–568. https://doi.org/10.1002/sus2.87

Yang K, Jia B, Liu J, Zhu K, Qin J, Jia H (2025) A novel perspective on the role of hydroxyl radicals in soil organic carbon mineralization within the detritusphere: stimulating C-degrading enzyme activities. Environ Sci Technol 59:5045–5055. https://doi.org/10.1021/acs.est.4c13619

Yu L, Bai J, Huang L, Zhang G, Wang W, Wang X, Yu Z (2021) Carbon-rich substrates altered microbial communities with indication of carbon metabolism functional shifting in a degraded salt marsh of the Yellow River Delta, China. J Clean Prod 331:129898. https://doi.org/10.1016/j.jclepro.2021.129898

Zhang X, Amelung W (1996) Gas chromatographic determination of muramic acid, glucosamine, mannosamine, and galactosamine in soils. Soil Biol Biochem 28:1201–1206. https://doi.org/10.1016/0038-0717(96)00117-4

Zhang P, Bing X, Jiao L, Xiao H, Li B, Sun H (2021) Amelioration effects of coastal saline-alkali soil by ball-milled red phosphorus-loaded biochar. Chem Eng J 431:133904. https://doi.org/10.1016/j.cej.2021.133904

Zhang G, Zhang L, Shi Z, Yang Y, Liu J (2025a) Microbial nutrient limitation and carbon use efficiency in saline-alkali soil amended with biochar: insights from ecoenzymatic C:N:P stoichiometry. Biochar 7:68. https://doi.org/10.1007/s42773-025-00458-y

Zhang Z, Bodenheimer J, Scott G, Dukes JS, Suseela V (2025b) Climatic stress-induced changes in plant chemistry alter the compound-specific degradation of litter during decomposition. New Phytol 248:92–106. https://doi.org/10.1111/nph.70449

Zhao Z, Zhou W (2019) Insight into interaction between biochar and soil minerals in changing biochar properties and adsorption capacities for sulfamethoxazole. Environ Pollut 245:208–217. https://doi.org/10.1016/j.envpol.2018.11.013

Zheng H, Wang X, Chen L, Wang Z, Xia Y, Zhang Y, Wang H, Luo X, Xing B (2018a) Enhanced growth of halophyte plants in biochar-amended coastal soil: roles of nutrient availability and rhizosphere microbial modulation. Plant Cell Environ 41:517–532. https://doi.org/10.1111/pce.12944

Zheng H, Wang X, Luo X, Wang Z, Xing B (2018b) Biochar-induced negative carbon mineralization priming effects in a coastal wetland soil: roles of soil aggregation and microbial modulation. Sci Total Environ 610–611:951–960. https://doi.org/10.1016/j.scitotenv.2017.08.166